

# First isolation and characterization of the prototype strain of the SARS-CoV-2 virus at the beginning of the COVID-19 pandemic in Peru

Primer aislamiento y caracterización de la cepa prototipo del virus

SARS-CoV-2 a inicios de la pandemia de la COVID-19 en el Perú

María P. García <sup>1,a</sup>, Miryam Palomino-Rodriguez <sup>2,b</sup>, Marcos Hernández <sup>2,c</sup>, Pamela Rios-Monteza <sup>2,d</sup>, Maribel Huaranga-Nuñez <sup>2,e</sup>, Carolina Guevara <sup>3,f</sup>, Jannet Otárola <sup>4,g</sup>, C. Padilla-Rojas <sup>5,h</sup>, Orson Mestanza <sup>5,i</sup>, Ronnie Gustavo Gavilán <sup>6,j</sup>, Nancy Merino-Sarmiento <sup>1,k</sup>, Gabriel De Lucio-Burga <sup>1,l</sup>, César Cabezas <sup>7,m</sup>

<sup>1</sup> National Reference Laboratory for Viral Metaxenics, National Center for Public Health – INS

<sup>2</sup> National Reference Laboratory for Respiratory Viruses, National Center for Public Health – INS

<sup>3</sup> Tropical Disease Research Center, NAMRU-6, Lima, Peru

<sup>4</sup> National Cell Culture Reference Laboratory, National Center for Public Health – INS

<sup>5</sup> National Reference Laboratory for Biotechnology and Molecular Biology, National Center for Public Health – INS

<sup>6</sup> National Reference Laboratory for Enteropathogens, National Center for Public Health – INS

<sup>7</sup> National Center for Public Health – INS

<sup>a</sup> Medical technologist. ORCID: 0000-0002-2185-5038

<sup>b</sup> Biologist, doctor of sciences. ORCID: 0000-0002-1236-4114

<sup>c</sup> Biologist, master in biological Sciences. ORCID: 0000-0002-5158-0450

<sup>d</sup> Biologist. ORCID: 0000-0002-2488-4686

<sup>e</sup> Medical technologist. ORCID: 0000-0001-9247-4040

<sup>f</sup> Biologist, master in microbiology. ORCID: 0000-0001-5112-6074

<sup>g</sup> Biologist. ORCID: 0000-0002-1482-7223

<sup>h</sup> Biologist. ORCID: 0000-0002-0562-0431

<sup>i</sup> Biologist, master in bioinformatics. ORCID: 0000-0001-7268-0496

<sup>j</sup> Biologist, doctor in molecular biology, ORCID: 0000-0003-1437-5607

<sup>k</sup> Medical technologist. ORCID: 0000-0002-4935-063X

<sup>l</sup> Biologist. ORCID: 0000-0002-8565-4331

<sup>m</sup> Infectious disease doctor. ORCID: 0000-0001-5120-0713

An Fac med. 2023;84(1):55-62. / DOI: <https://doi.org/10.15381/anales.v84i1.24134>.

## Corresponding author:

María Paquita García Mendoza  
pgarcia@ins.gob.pe

Received: 29 November 2022

Accepted: 15 January 2023

Online publication: 28 February 2023

**Conflicts of interest:** All authors declare that they have no conflicts of interest.

**Funding source:** This study was funded by the National Institute of Health (registration code OC-026-20).

**Authorship contributions:** Authorship contributions: All authors participated in the conception, design of the article and data collection, interpretation of the data, writing of the manuscript, critical review of the manuscript, and approval of the final version. They all assume responsibility for what is published.

**Cite as:** García M, Palomino-Rodriguez M, Hernandez M, Rios-Monteza P, Huaranga-Nuñez M, Guevara C, et al. First isolation and characterization of the prototype strain of the SARS-CoV-2 virus at the beginning of the COVID-19 pandemic in Peru. *An Fac med.* 2023;84(1):55-62. DOI: <https://doi.org/10.15381/anales.v84i1.24134>

## Abstract

**Introduction:** Currently, isolated from SARS-CoV-2 virus exceed 600 million cases in the world. **Objective:** Isolation and characterization of the SARS-CoV-2 virus causing COVID-19 at the beginning of the pandemic in Peru. **Methods:** Twenty nasal and pharyngeal swab samples were isolated from SARS-CoV-2 using two cell lines, Vero ATCC CCL-81 and Vero E-6; virus identification was performed by RT-PCR and the onset of cytopathic effect (CPE) was evaluated by indirect immunofluorescence and subsequent identification by genomic sequencing. One of the most widely circulating isolates were selected and named the prototype strain (PE/B.1.1/28549/2020). Then 10 successive passages were performed on Vero ATCC CCL-81 cells to assess mutation dynamics. **Results:** Results detected 11 virus isolates by cytopathic effect, and subsequently confirmed by RT-PCR and indirect immunofluorescence. Of these, six were sequenced and identified as the lineages B.1, B.1.1, B.1.1.1, and B.1.205 according to the Pango lineage nomenclature. The prototype strain corresponded to lineage B.1.1. The analysis of the strains from the successive passages showed mutations mainly at in the spike (S) protein of the virus without variation in the identity of the lineage. **Conclusions:** Four lineages were isolated in the Vero ATCC CCL-81 cell line. Subcultures in the same cell line showed mutations in the spike protein indicating greater adaptability to the host cell and variation in pathogenicity *in vitro*, a behavior that allows it to have more survival success.

**Keywords:** Coronavirus Infections; Betacoronavirus; Vero Cells; Virulence (Source: MeSH).

## Resumen

**Introducción:** Actualmente los contagios por el virus del SARS-CoV-2 supera los 600 millones de casos en el mundo. **Objetivo:** Aislar y caracterizar el virus SARS-CoV-2 causante de la COVID-19 a inicios de la pandemia en el Perú. **Métodos:** Se realizó el aislamiento viral a partir de 20 muestras de hisopado nasal y faríngeo positivas a SARS-CoV-2 por RT-PCR. El aislamiento se realizó en las líneas celulares Vero ATCC CCL-81 y Vero E6, evaluando el efecto citopático, la presencia del virus por RT-PCR, inmunofluorescencia indirecta (IFI) y posterior identificación por secuenciación genómica. Posteriormente, uno de los aislamientos de mayor circulación fue seleccionado y denominado cepa prototipo (PE/B.1.1/28549/2020), realizándose 10 pasajes sucesivos en células Vero ATCC CCL-81 para evaluar la dinámica de mutaciones. Resultados: Se observaron 11 aislamientos de virus por efecto citopático confirmándose por RT-PCR e IFI, de los cuales 6 fueron secuenciados identificándose los linajes B.1, B.1.1, B.1.1.1 y B.1.205, según el comité Pango de los genomas. La cepa prototipo corresponde a la variante B.1.1 y el análisis de las secuencias de los pasajes sucesivos mostró mutaciones a nivel de la proteína de la espiga (S) del virus, sin variación en la identidad del linaje. **Conclusiones:** Se aislaron 4 linajes en la línea celular Vero ATCC CCL-81. Los subcultivos en la misma línea celular muestran mutaciones en la proteína de la espiga, lo que indica mayor adaptabilidad a la célula hospedera y variación de la patogenicidad *in vitro*, comportamiento que le permite tener más éxito de supervivencia.

**Palabras clave:** Infecciones por Coronavirus; Betacoronavirus; Células Vero; Virulencia (fuente: DeCS BIREME)

## INTRODUCTION

At the end of December 2019, in the city of Wuhan in the People Republic of China, the new coronavirus known as SARS-CoV-2 appeared, which is the cause of the new disease called COVID-19<sup>(1)</sup>. This new respiratory virus quickly spread to many countries and caused cases of atypical pneumonia, which in association with a series of risk factors, generated cases of greater severity and mortality<sup>(2,3)</sup>. On March 11, 2020, the infection was declared a pandemic by the World Health Organization (WHO)<sup>(4)</sup>.

In Peru, the National Institute of Health reported the first confirmed case of COVID-19 on March 6, 2020. Despite the strict measures of social immobilization adopted by the government, cases of infection by SARS-CoV-2 were increasing considerably, the highest peak of infection of the first wave was in July 2020. Peru was the country with the highest mortality rate per capita in the world<sup>(5)</sup>.

The constant genetic mutations of the SARS-CoV-2 virus have led to the emergence of various variants that have spread throughout the world<sup>(6)</sup>, observing evolutionary competition between them, with the displacement of one over the other. These mutations are responsible for the various peaks of contagion observed in all countries<sup>(7,8)</sup>. According to their impact on public health, the World Health Organization (WHO) has classified them into variants of concern (VOCs) and

variants of interest (VOIs)<sup>(9)</sup>. Currently, variants with low levels of circulation or not detected are classified as variants of low monitoring, while omicron belongs to the VOC and VOI.

Peru has registered four waves; the first in April 2020 generated by the B.1.1 variant as the predominant lineage<sup>(10,11)</sup>; the second wave during the first half of 2021 was caused by the lambda/gamma variant (C37/P1)<sup>(12)</sup>; the third wave in January 2022 was caused by the omicron variant, mainly (BA.1/BA.2)<sup>(12,13)</sup>; and the fourth wave in June 2022 was caused by the sublineages/subvariants of omicron (BA.4 and B.A.5)<sup>(13,14)</sup>.

The isolation, typing, characterization of the behavior of the virus, and the determination of the humoral response to natural infection and vaccination are scientific achievements derived from knowledge of virus biology. Among the applications of the isolation of the SARS-CoV-2 virus we have the elaboration of quality assessment panels to guarantee the molecular diagnosis of SARS-CoV-2; the evaluation of active principles with potential therapeutic; and the development of various test methods such as immunoenzymatic tests that detect IgM and IgG antibodies, the plaque reduction neutralization test (PRNT) for titration of neutralizing antibodies, and indirect immunofluorescence (IFA) for the detection of viruses and total antibodies. Therefore, this study aimed to isolate and characterize the SARS-CoV-2 virus from nasal

and pharyngeal swab samples obtained at the beginning of the COVID-19 pandemic in Peru.

## METHODS

### Samples

Twenty nasal and pharyngeal swab samples with positive results according to the RT-PCR method for SARS-CoV-2<sup>(15)</sup>. Cycle threshold (Ct) values of less than 30 were considered for an adequate viral load<sup>(16)</sup>. The samples were received by the National Reference Laboratory for Respiratory Viruses (LRNVR) of the National Institute of Health (INS) (Lima-Peru) in April 2020. The summary of the isolation and identification of the prototype strain is shown in Figure 1.

### Cell culture

The Vero ATCC CCL-81 and E6 cell lines were used for the isolation of the SARS-CoV-2 virus<sup>(17,18)</sup>. Cells were grown in Earle's minimal essential medium (EMEM) supplemented with 10% fetal bovine serum (FBS, SIGMA brand) and 1% penicillin-streptomycin-amphtericin, and cultured at 37°C in a humidified atmosphere containing 5% CO<sub>2</sub><sup>(18)</sup>.

### Isolation and passage of the SARS-CoV-2 virus

The isolation of the SARS-CoV-2 virus was carried out in the facilities of the biosafety

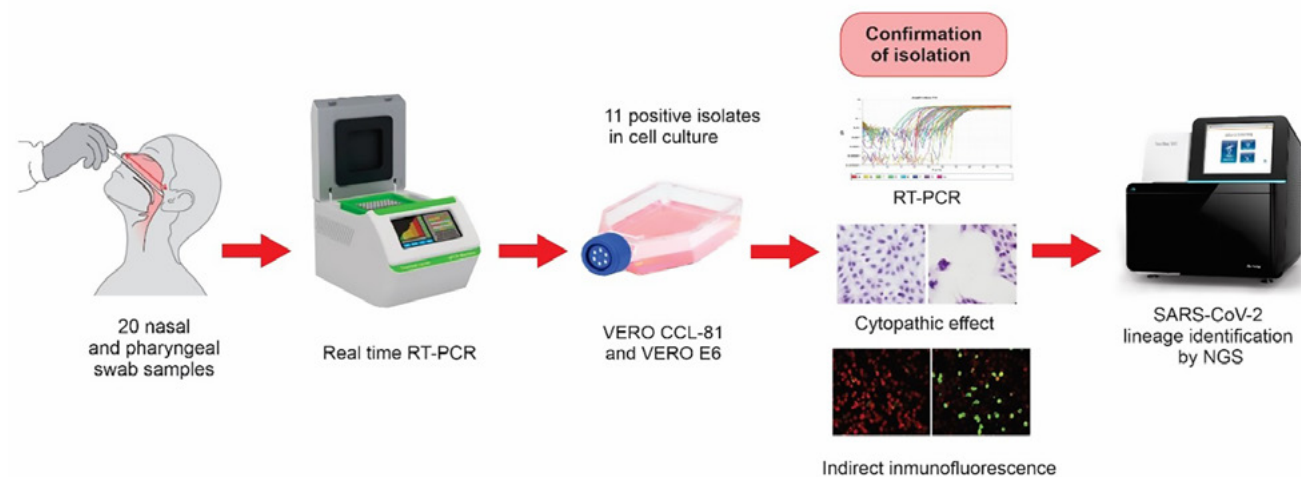


**Figure 1.** Graphic summary of the isolation and identification of the prototype strain (PE/B.1.1/28549/2020) of SARS-CoV-2 at the beginning of the pandemic in Peru.

level 3 (BSL-3) laboratory of the Microbiology and Biomedicine Laboratory of the INS. International established protocols<sup>(19)</sup> and institutional procedures for the isolation of respiratory viruses<sup>(20)</sup> were followed. The swab samples positive for SARS-CoV-2 were filtered with a 0.22 µm pore membrane and inoculated into the Vero ATCC CCL-81 and E6 cell line with 90% cell confluence, after 1 hour of viral adsorption at 37°C, 3 mL of EMEM medium with 2% SBF were added and incubated at 37°C at 5% CO<sub>2</sub>. The cells were observed daily under an inverted microscope to detect the appearance of a cytopathic effect, up to seven days after infection<sup>(21,22)</sup>. The supernatants were collected for RT-PCR confirmation, and adherent cells were used for confirmation by IFA.

### Viral quantification

The quantification of the SARS-CoV-2 virus was carried out using the plaque assay. Twenty-four-well flat-bottom cell culture plates were used; the plates were seeded with a cell suspension of 2.5 x 10<sup>5</sup>/mL cells (Vero ATCC CCL-81) and incubated at 37 °C with 5% CO<sub>2</sub> overnight to achieve 100% confluence<sup>(23)</sup>.

The cells were infected with the virus by performing serial tenfold dilutions (10<sup>-1</sup>, 10<sup>-2</sup>, 10<sup>-3</sup>, 10<sup>-4</sup>, 10<sup>-5</sup>, and 10<sup>-6</sup>) and incubated at 37 °C with 5% CO<sub>2</sub> for 60 min. Subsequently, 1 mL of overlay medium (2X MEM medium supplemented with 2 nM L-glutamine), 10% fetal bovine serum, 100 units/mL of antibiotic, and carboxymethylcellulose (SIGMA CMC at 3%) were added to each well. The cells were incubated at 37°C with 5% CO<sub>2</sub>. After five days, the medium was removed, the cells were fixed and stained with crystal violet/formaldehyde. The titers of SARS-CoV-2 were expressed as plaque-forming units per milliliter (PFU/mL)<sup>(24,25)</sup> Latin American (LA).

### Viral confirmation tests

#### Detection of SARS-CoV-2 by real-time RT-PCR

Briefly, 200 µL of the culture supernatant were collected, which was inactivated at 56°C and 450 rpm in a thermoblock for 60 min<sup>(26)</sup>. Then it was transported to

the biosafety level 2 (BSL-2) laboratory. RNA extraction was performed using the Zymo nucleic acid viral extraction kit (China), through the magnetic bead method, following the manufacturer's instructions<sup>(22,27)</sup> 2019. Purified RNA samples were processed by RT-PCR. The amplification process was performed using the SuperScript™ IV one-step kit (Invitrogen) following standardized conditions<sup>(15,28)</sup>. The predictive positive and negative values (PPV and PNV, respectively).

#### Indirect immunofluorescence complementary test

The indirect immunofluorescence (IFA) technique was developed to detect the SARS-CoV-2 virus isolated in cell culture. Serum sample from a convalescent patient (positive diagnosis for SARS-CoV-2 by RT-PCR), characterized by the plaque reduction neutralization test (PRNT), was used as a source of polyclonal antibodies to the SARS-CoV-2 virus.

Briefly, seven days after the infection of the Vero ATCC CCL-81 and Vero E6 cells, the supernatant was collected and the cells were washed and homogenized with PBS 1X. An appropriate cell suspension was obtained and dispensed into immunofluorescence slides, these slides were fixed with acetone -20 °C/20 min; for virus detection, 20 µL of a serum dilution (positive control serum, negative control serum at 1/20 dilution in PBS) and PBS diluent control were added in duplicate, and incubated in a humid chamber at 37 °C/30 min, washed twice with PBS and left to dry at room temperature; subsequently, 20 µL of FITC (fluorescein isothiocyanate)-labeled anti-human IgG conjugate + Evans Blue (100X) in a dilution of (1/160) was added to all the wells and incubated in a humid chamber at 37°C/30 min protected from light, washed twice with PBS and the mounting medium was added, pH 7.2- 7.4<sup>(22,27)</sup>. The reading was carried out under a fluorescence microscope; the slides can be kept for up to 24 h at 4 °C in the dark. The interpretation is based on the presence of

fluorescence (positive), the absence of fluorescence is considered negative.

#### In vitro evolutionary dynamics model and characterization

The Dynamics of Viral Evolution Model Proposed by Wood<sup>(29)</sup> was used, which suggests 10 successive passages in culture of the same cell line to know the adaptation of the virus to the new host environment in relation to virulence. From the isolation of one of the positive samples, which we call prototype strain (PE/B.1.1/28549/2020), 10 continuous passages were made in the Vero ATCC CCL-81 cell line. The culture of the virus in each passage was observed until the appearance of the cytopathic effect (5 to 7 days). The supernatant was collected and centrifuged at 2000 rpm for 10 min at 4°C and aliquots were taken for viral titration and genomic sequencing analysis.

#### Whole genome sequencing of SARS-CoV-2 isolates

The samples of the isolates and passages of the prototype strain (PE/B.1.1/28549/2020) of the SARS-CoV-2 virus were extracted using the MAGBEAD viral DNA/RNA extraction kit (ZymoBIOMICS) on the automated OpenTrons OT-2 platform. The library preparation was performed using the COVIDSeq test from Illumina and sequenced on NextSeq 550 (Illumina®) following the manufacturer's instructions<sup>(30)</sup>.

#### Bioinformatic analysis

The quality of the reads and the removal of read contamination were performed using FastQC v0.11.9 (<https://www.bioinformatics.babraham.ac.uk/projects/fastqc/>), and Kraken2 v2.0.8 respectively<sup>(29)</sup>. The filtered reads were assigned to the NCBI reference sequence (NC\_045512) isolated from Wuhan through the BWA software package v0.7.17<sup>(31)</sup>. The consensus sequence was obtained using Samtools v.1.9 and iVar v.1<sup>(32,33)</sup>. Finally, the annotation of the consensus sequences was performed using Next-

Clade (<https://clades.nextstrain.org/>), and the lineage designation was defined using Pangolin v.3.1.2 software (<https://pangolin.cog-uk.io/>). The summary of mutation was calculated using the Snipit program (<https://github.com/aineniameh/snipit>) with manual editing, the first isolate was used as reference. The genomes were aligned with the MAFFT v7.310 program (<https://mafft.cbrc.jp/alignment/software/>) against the SARS-CoV-2 reference (NC\_045512). The multiple alignment was used for the phylogenetic inference of the isolates, this was calculated with the RaxML v8.2.12 program <sup>(34)</sup> with 1000 bootstrap.

## RESULTS

### Viral isolation and cytopathic effect (CPE)

The SARS-CoV-2 virus was isolated in two cell lines Vero ATCC CCL-81 and Vero E6. The assessment of viral infection was carried out by observing the cytopathic effect (CPE). Faster viral replication was observed in Vero ATCC CCL-81 cells than in Vero E6 cells, from the third day after infection. The CPE in Vero ATCC CCL-81 cells was characterized by round cell foci on the surface of the monolayer cell, expanding to a gradual and homogeneous detach-

ment. Vero E6 cells showed formation of syncytia and detachment only in some samples, with slow development of CPE from the 3 days after infection.

Vero ATCC CCL-81 cells were optimal for the isolation of the SARS-CoV-2 virus, due to their more homogeneous and characteristic viral replication phenotype. Figure 2 shows the comparative CPE between Vero ATCC CCL-81 and Vero E6 cells after 3 and 5 days after infection, with the same swab sample. The round cells and syncytia were observed, respectively, compared to the monolayer of the control cells.

### Confirmation of Isolation by RT-PCR and IFA

Eleven (55.0%) isolations of 20 nasopharyngeal and pharyngeal swab samples were confirmed by RT-PCR method, from the cell line Vero ATCC CCL-81 cultures. The Ct values of the isolations were found in the range of 11 to 14, indicating that there was viral replication compared to the initial Ct of the diagnostic RT-PCR (Ct <30).

The IFA confirmed the same 11 (55.0%) isolations in the 20 nasopharyngeal and pharyngeal swab samples,

without differences between the two Vero ATCC CCL-81 and Vero E6 cell lines. Figure 3 shows the identification of the SARS-CoV-2 virus isolation by IFA in Vero ATCC CCL-81 cells, observing the control cells without infection (red) and the cells infected with the SARS-CoV-2 virus with fluorescence (green).

The sample with code 28549 was highlighted, whose isolation was one of those that presented lower Ct values, indicating a high viral load, in addition to showing the characteristic CPE and confirmation by IFA. This was selected as a prototype strain and named PE/B.1.1/28549/2020 (Table 1).

### Sequencing of the complete genome of SARS-CoV-2 samples and phylogenetic analysis

Of the 11 samples with confirmed isolation of the SARS-CoV-2 virus, the complete genome of 6 samples was obtained, which were analyzed and classified into 4 different PANGO lineages (one B.1, one B.1.1, two B.1.1.1 and two B.1.205). The lineage of the prototype strain PE/B.1.1/28549/2020 corresponds to B.1.1 (Table 1). The phylogenetic analysis shows the genetic distances between the different lineages isolated at the beginning of the pandemic compared to the basal NC\_045512.2 (Figure 4).

### In vitro evolutionary dynamics

The successive passages of the prototype strain PE/B.1.1/28549/2020 show the adaptation of the SARS-CoV-2 virus in the Vero ATCC CCL-81 cell line, with a progressive increase in the viral titer with a higher number of passages and a subsequent decrease in the last passages (Figure 5A). This adaptation shows the progressive increase in virulence in the Vero ATCC CCL-81 cell line, observed from the formation of deficient plaque-forming units (PFU), with undefined edges in the first passages, which progressively define in passages 3 and 4; while in passage 8 translucent, circular and symmetrical lysis plates with regular edges are shown (Figure 5B). The quantification of the PFU shows the progressive increase in the viral titer proportional to the number of passages, with a peak in

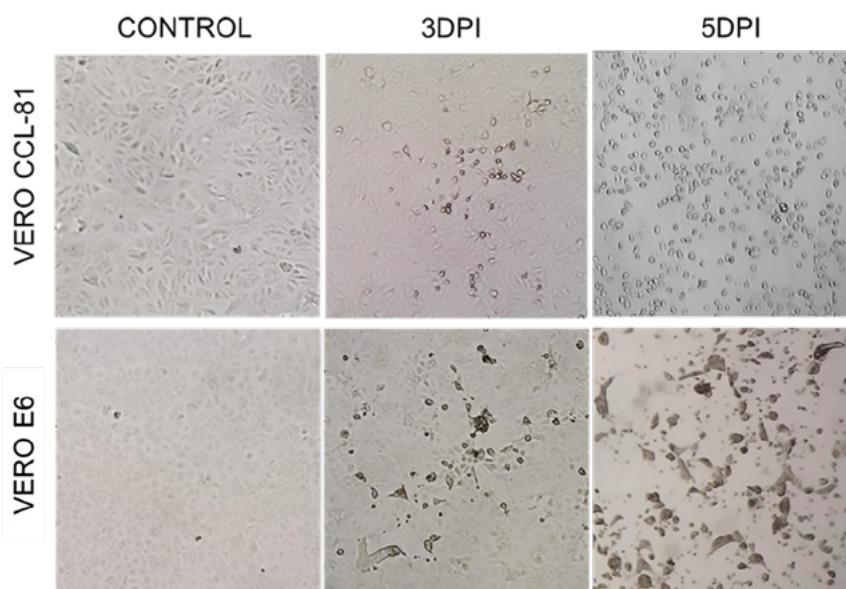


**Figure 2.** Comparative cytopathic effect in Vero ATCC CCL-81 and Vero E6 cell lines infected with the SARS-CoV-2 virus. The morphology in cells is shown at 3 and 5 days post infection (DPI).

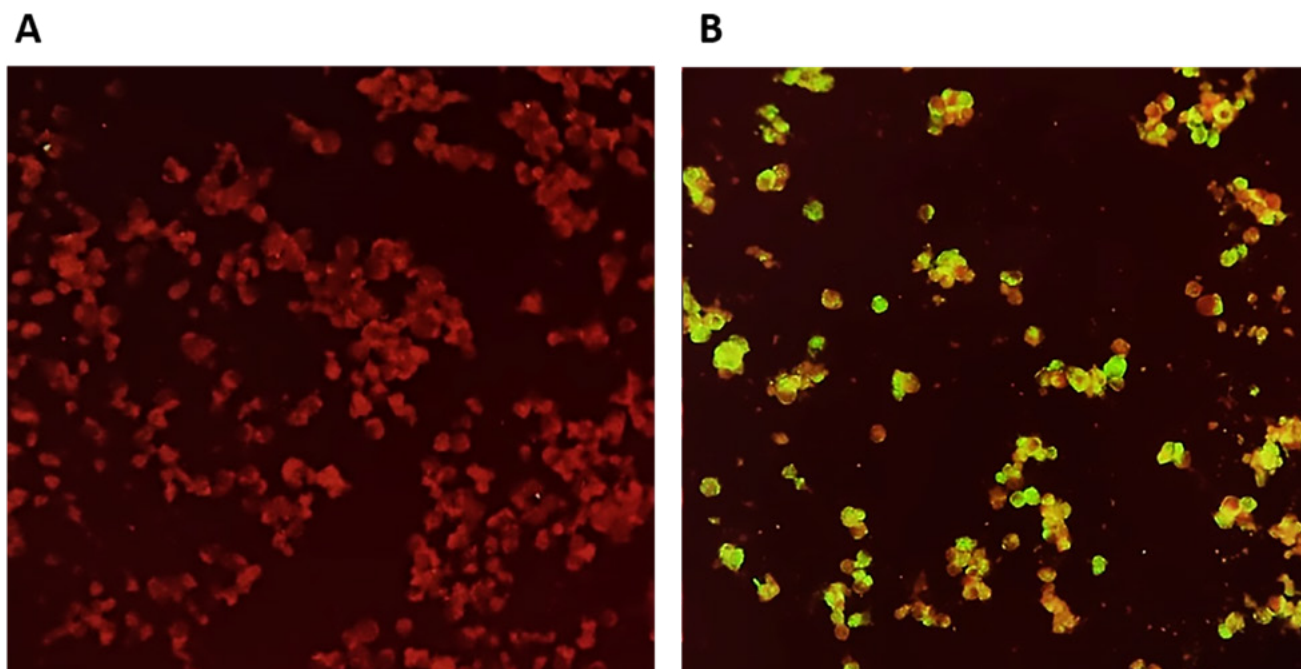


**Figure 3.** Identification of SARS-CoV-2 virus isolation by indirect immunofluorescence test (IFA). A. Negative reaction for IFA. B. Positive reaction for IFA.

passage 7 with an average of  $59.5 \times 10^5$  PFU/mL and subsequent decline in the following passages (Figure 5C).

In complement to the phenotypic characteristics observed in the passages of the prototype strain, sequencing in

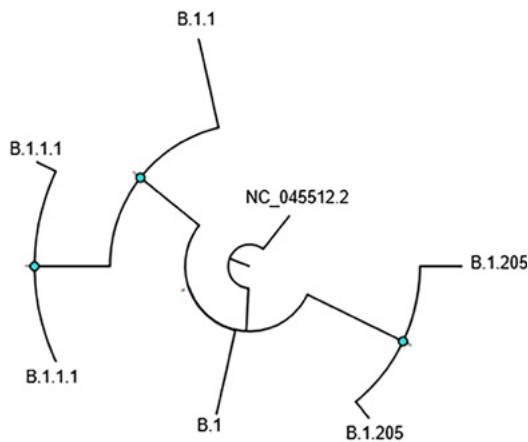
each passage showed alterations in the genome of the lineage associated with the phenotype and viral load (Figure 6).

**Table 1.** Result of diagnosis, isolation and sequencing of the 20 SARS-CoV-2 samples.

Sample		Swab sample (nasal and pharyngeal)		Confirmatory tests for viral isolation				Sequencing
N°	Sample code	RT-PCR		RT-PCR of the isolate on Vero ATCC CCL-81		Vero ATCC CCL-81 and Vero E-6		NGS
		Ct	Result	Ct	Result	Cytopathic effect	IFA	Linage (PANGO)
1	28549	21.42	Positive	9.56	Positive	Positive	Positive	B.1.1
2	28594	20.56	Positive	10.45	Positive	Positive	Positive	B.1.1.1
3	08720	19.07	Positive	13.63	Positive	Positive	Positive	*
4	25413	16.04	Positive	12.93	Positive	Positive	Positive	B.1.1.1
5	09116	22.30	Positive	12.89	Positive	Positive	Positive	*
6	27171	23.70	Positive	33.61	Negative	Negative	Negative	-
7	27148	28.52	Positive	36.63	Negative	Negative	Negative	-
8	25400	20.30	Positive	12.51	Positive	Positive	Positive	*
9	28755	20.79	Positive	10.05	Positive	Positive	Positive	*
10	27195	23.58	Positive	35.43	Negative	Negative	Negative	-
11	28782	16.83	Positive	12.27	Positive	Positive	Positive	B.1.205
12	25618	29.97	Positive	37.04	Negative	Negative	Negative	-
13	25480	28.40	Positive	38.43	Negative	Negative	Negative	-
14	29700	21.54	Positive	10.80	Positive	Positive	Positive	B.1.205
15	25303	21.81	Positive	31.91	Negative	Negative	Negative	-
16	25142	24.03	Positive	10.59	Positive	Positive	Positive	B.1
17	284674	22.23	Positive	10.71	Positive	Positive	Positive	*
18	28520	19.38	Positive	29.92	Negative	Negative	Negative	-
19	23611	24.95	Positive	35.98	Negative	Negative	Negative	-
20	25262	22.19	Positive	33.05	Negative	Negative	Negative	-

\*Not sequenced due to insufficient sample.

NGS: Next Generation Sequencing, RT-PCR: Reverse transcription PCR, IFA: Indirect Immunofluorescence Assay



N°	Code	ID access	Collection date	Lineage
1	29700	EPI_ISL_1111169	15/04/2020	B.1.205
2	28594	EPI_ISL_1111367	13/04/2020	B.1.1.1
3	25142	EPI_ISL_1111376	12/04/2020	B.1
4	28782	EPI_ISL_1111374	14/04/2020	B.1.205
5	28549	EPI_ISL_1111366	13/04/2020	B.1.1
6	25413	EPI_ISL_1111368	12/04/2020	B.1.1.1

**Figure 4.** Phylogeny of SARS-CoV-2 virus lineages isolated in April 2020 in Lima- Peru at the beginning of the pandemic.

In passage 2 (P2) of the prototype strain, a 27-base pair deletion was found at position 21764- 21790 and mutations at the spike protein level in passage 4 (P4)

and passage 8 (P8). The mutation of passage 4 at position 23014 corresponds to an amino acid change from glutamic acid to aspartic acid (E484D) and the second

mutation at position 24507 corresponds to the change of a serine to leucine (S982L).

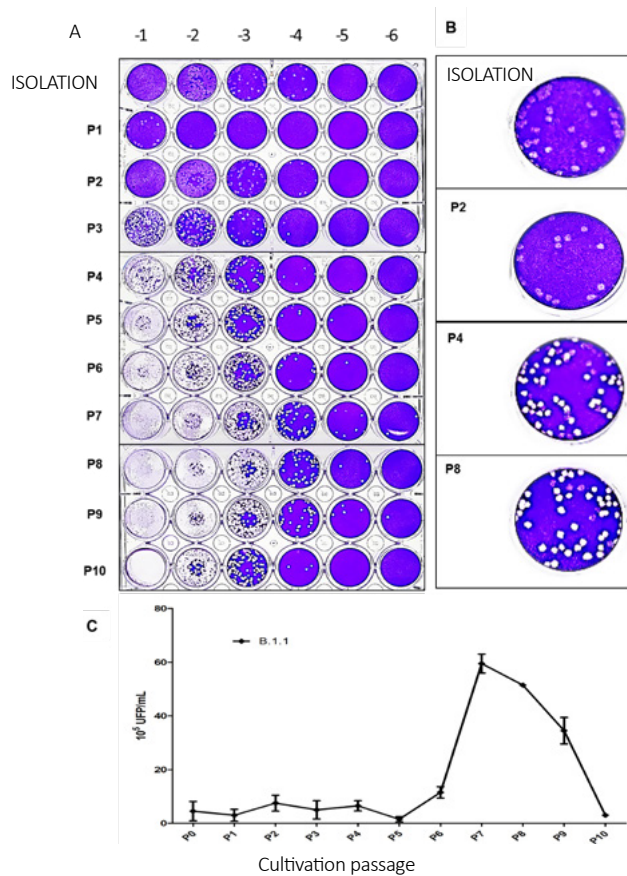


**Figure 5.** Mutational dynamics of the B.1.1 lineage of SARS-CoV-2 (PE/B.1.1/28549/2020) in 10 successive passages in Vero ATCC CCL-81 cells. A. Titration of the 10 passages of the SARS-CoV-2 virus. B. Morphological aspect of the viral plates of the passages of the SARS-CoV-2 virus. C. Quantification of the viral titer in the 10 passages. The data show the mean and standard deviation of 4 replicates.

**DISCUSSION**

Our results are in agreement with other reports that mention the higher probability of SARS-CoV-2 virus isolation associated with the viral load of the samples, with Ct <24 achieving 80% virus recovery<sup>(35)</sup>. The usefulness of the Vero ATCC CCL-81 and Vero E6 cell lines in the replication of the SARS-CoV-2 virus is also shown, with preference for the Vero ATCC CCL-81 cell as reported by some studies<sup>(36)</sup>, unlike others that indicate greater cell replication in Vero E6, being the most used<sup>(17)</sup>. For this study, the classic isolation was used, which is still a standard of comparison, although currently automated high-speed large-scale SARS-CoV-2 isolation methods have been developed from clinical samples by miniaturized co-culture<sup>(37)</sup>.

In this research, the isolation of the SARS-CoV-2 virus from 11 nasopharyngeal and pharyngeal swab samples was confirmed by the RT-PCR and IFA methods. It was observed that in the RT-PCR of the isolation, Ct values were lower compared to the diagnostic RT-PCR. The 9 non-isolated samples - despite having a positive isolation RT-PCR- the Ct values are higher than the diagnostic PCR, which indicates that there was no viral replication, this was

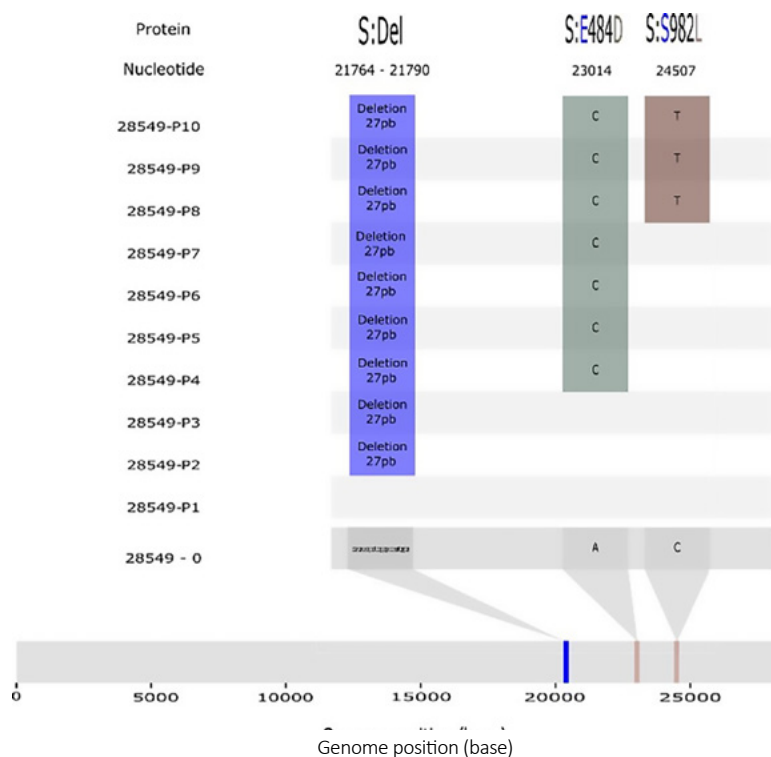


**Figure 6.** Sequencing of the 10 passages of the B.1.1 lineage of the SARS-CoV-2 virus. A deletion of 27 base pairs at position 21764 - 21790 is observed in passage 2 (P2) and mutations at the level of the spike protein in passage 4 (P4) at position 23014 (E484D) and passage 8 (P8) corresponds to position 24507 (S982L).

complemented with the negative results of the cytopathic effect and IFA.

The selection of the prototype strain of the SARS-CoV-2 virus named PE/B.1.1/28549/2020 and the generation of 10 successive *in vitro* passages showed mutations of the virus for better adaptation to the Vero ATCC CCL-81 host cell, in this case, specifically at the spike protein level, causing deletions and mutations. The nucleotide mutation of passage 4 (P4) at position 23014 (E484D) allowed the strain to adapt to the cell line and successfully infect, with an increase in its virulence. This mutation was reported in the original strain from Wuhan (Wuhan-Hu-1, GenBank accession number NC\_045512)<sup>(38)</sup>.

The second mutation of passage 8 corresponds to position 24507 (S982L), this mutation decreases its virulence, but demonstrates the genetic adaptation to the cell line. Research with similar results indicates that the SARS-CoV-2 virus when cul-

tivated is under strong selective pressure to acquire these mutations in various ORFs of the genome, including the S gene<sup>(39,40)</sup>. These findings confirm that these mutations are fixed during the adaptation of the virus to the conditions of the environment, as shown by *in vitro* RNA studies<sup>(40,41)</sup>.

In conclusion, the SARS-CoV-2 virus was isolated in Vero ATCC CCL-81 cells. The isolation was performed from samples obtained during the first wave of the COVID-19 pandemic in Peru. In April 2020, four PANGO lineages (B.1, B.1.1, B.1.1.1 and B.1.205) were identified. The successive passages of the prototype strain PE/B.1.1/28549/2020 showed mutations in the spike protein indicating its adaptation to the host cell, which allows it to have greater survival success. The obtaining of this isolate allowed us to transfer the biological material to other research institutions that were developing technologies to face the COVID-19 pandemic.

**Acknowledgments:** The authors thank the COVID-19 diagnostic team of the National Health Institute of Peru and the coordination staff of the Respiratory Virus Laboratory, Blga. Nancy Rojas, Blgo. Joseph Huayra, Blga. Gloria Arotinco and Blga. Priscilla Lopez. In addition, we thank the collaboration of the Center for Research on Tropical Diseases, NAMRU-6, to Dr. Max Groggl, TM. Dina Popuche and Lab. Technician Alfredo Huamán.

## REFERENCES

1. World Health Organization. WHO Director-General's remarks at the media briefing on 2019-nCoV on 11 February 2020 [Internet]. 2020 [cited 2022 May 26]. Available from: <https://www.who.int/director-general/speeches/detail/who-director-general-s-remarks-at-the-media-briefing-on-2019-ncov-on-11-february-2020>
2. Huang D, Lian X, Song F, Ma H, Lian Z, Liang Y, et al. Clinical features of severe patients infected with 2019 novel coronavirus: a systematic review and meta-analysis. *Ann Transl Med.* 2020; 8(9):576-576. doi:10.21037/ATM-20-2124
3. Wu F, Zhao S, Yu B, Chen YM, Wang W, Song ZG, et al. A new coronavirus associated with human respiratory disease in China. *Nature.* 2020; 579(7798):265-269. doi:10.1038/s41586-020-2008-3
4. Organización Panamericana de la Salud. La OMS caracteriza a COVID-19 como una pandemia - OPS/OMS | Organización Panamericana de la Salud [Internet]. 2020 [cited 2022 Sep 5]. Available from: <https://www.paho.org/es/noticias/11-3-2020-oms-caracteriza-covid-19-como-pandemia>
5. BBC News Mundo. Perú duplica las muertes por covid-19 tras una revisión de cifras y se convierte en el país con la mayor tasa de mortalidad per cápita del mundo - BBC News Mundo [Internet]. 2021 [cited 2022 Sep 5]. Available from: <https://www.bbc.com/mundo/noticias-america-latina-57310960>
6. CDC. Clasificaciones y definiciones de las variantes del SARS-CoV-2 [Internet]. 2021 [cited 2021 Oct 16]. Available from: <https://espanol.cdc.gov/coronavirus/2019-ncov/variants/variant-info.html>
7. Phan T. Genetic diversity and evolution of SARS-CoV-2. *Infect Genet Evol.* 2020; 81:104260. doi:10.1016/j.meegid.2020.104260
8. Johns Hopkins University Medicine. COVID-19 Map - Johns Hopkins Coronavirus Resource Center [Internet]. 2022 [cited 2022 Jul 5]. Available from: <https://coronavirus.jhu.edu/map.html>
9. Organización Mundial de la Salud (OMS). Seguimiento de las variantes del SARS-CoV-2 [Internet]. 2022 [cited 2022 Jul 5]. Available from: <https://www.who.int/es/activities/tracking-SARS-CoV-2-variants>
10. Gutiérrez-Tudela JW. La pandemia de la COVID-19 en el Perú: análisis epidemiológico de la primera ola. *Rev la Soc Peru Med Interna.* 2021; 34(2):51-2. doi:10.36393/SPMI.V34I2.595
11. Padilla-Rojas C, Vega-Chozo K, Galarza-Perez M, Bailon Calderon H, Lope-Pari P, Balbuena-Torres J, et al. Genomic analysis reveals local transmission of SARS-CoV-2 in early pandemic phase in Peru. *bioRxiv.* 2020; 2020.09.05.284604. doi:10.1101/2020.09.05.284604
12. Toyama M, Vargas L, Ticlihuana S, Quispe AM. Regional clustering and waves patterns due to COVID-19

- by the index virus and the lambda/gamma, and delta/omicron SARS-CoV-2 variants in Peru. *Ann Epidemiol.* 2022; 75:74. doi:10.1016/j.annepidem.2022.08.026
13. Ministerio de salud Perú. Sala de Situación de COVID-19 [Internet]. 2022 [cited 2022 Apr 28]. Available from: <https://www.dge.gob.pe/covid19.html>
  14. Lupa S con. Perú entró en la cuarta ola de covid-19 con más de 11.000 casos semanales - Salud con lupa [Internet]. 2022 [cited 2022 Jul 5]. Available from: <https://saludconlupa.com/noticias/peru-entro-en-la-cuarta-ola-de-covid-19-con-mas-de-11000-casos-semanales/>
  15. Rojas-Serrano N, Lope-Pari P, Huaranga-Núñez M, Simas PVM, Palacios-Salvatierra R, Balbuena-Torres J, *et al.* Validación y evaluación de una prueba de RT-PCR en tiempo real in house para la detección de SARS-CoV-2 usando un gen específico RdRp y control endógeno GAPDH. *Rev Peru Med Exp Salud Publica.* 2021; 38(4):595-600. doi:10.17843/RPMESP.2021.384.7596
  16. Padilla-Rojas C, Jimenez-Vasquez V, Hurtado V, Mestanza O, Molina IS, Barcena L, *et al.* Genomic analysis reveals a rapid spread and predominance of lambda (C.37) SARS-COV-2 lineage in Peru despite circulation of variants of concern. *J Med Virol.* 2021; 93(12):6845-9. doi:10.1002/JMV.27261
  17. Harcourt J, Tamin A, Lu X, Kamili S, Kumar Sakthivel S, Murray J, *et al.* Isolation and characterization of SARS-CoV-2 from the first US COVID-19 patient. *bioRxiv.* 2020; 2020.03.02.972935. doi:10.1101/2020.03.02.972935
  18. Yamada S, Fukushi S, Kinoshita H, Ohnishi M, Suzuki T, Fujimoto T, *et al.* Assessment of SARS-CoV-2 infectivity of upper respiratory specimens from COVID-19 patients by virus isolation using VeroE6/TMPRSS2 cells. *BMJ Open Respir Res.* 2021; 8(1). doi:10.1136/BMJRESP-2020-000830
  19. OMS. Criterios para poner fin al aislamiento de los pacientes de COVID-19: reseña científica, 17 de junio de 2020 [Internet]. 2020 [cited 2023 Feb 2]. Available from: <https://apps.who.int/iris/handle/10665/332997>
  20. Roth B, Mohr H, Enders M, Garten W, Gregersen JP. Isolation of influenza viruses in MDCK 33016PF cells and clearance of contaminating respiratory viruses. *Vaccine.* 2012; 30(3):517-22. doi:10.1016/j.vaccine.2011.11.063
  21. Taştan C, Yurtsever B, Sir Karakuş G, Dilek Kancağlı D, Demir S, Abanuz S, *et al.* SARS-CoV-2 isolation and propagation from Turkish COVID-19 patients. *Turk J Biol.* 2020; 44(3):192-202. doi:10.3906/biy-2004-113
  22. Díaz FJ, Aguilar-Jiménez W, Flórez-Álvarez L, Valencia G, Laiton-Donato K, Franco-Muñoz C, *et al.* Aislamiento y caracterización de una cepa temprana de SARS-CoV-2 durante la epidemia de 2020 en Medellín, Colombia. *Biomédica.* 2020; 40(Supl. 2):148-58. doi:10.7705/BIOMEDICA.5834
  23. Mendoza EJ, Manguiat K, Wood H, Drebort M. Two Detailed Plaque Assay Protocols for the Quantification of Infectious SARS-CoV-2. *Curr Protoc Microbiol.* 2020; 57(1):cpmc105. doi:10.1002/CPMC.105
  24. Leite JA, Resende P, Araya JL, Barrera GB, Baumeister E, Caicedo AB, *et al.* Genetic evolution of influenza viruses among selected countries in Latin America, 2017-2018. *PLoS One.* 2020; 15(3):e0227962. doi:10.1371/JOURNAL.PONE.0227962
  25. Harfoot R, Lawley B, Hernández LC, Kuang J, Grant J, Treece JM, *et al.* Characterization of the First SARS-CoV-2 Isolates from Aotearoa New Zealand as Part of a Rapid Response to the COVID-19 Pandemic. *Viruses.* 2022; 14(2):366. doi:10.3390/V14020366/S1
  26. Jureka AS, Silvas JA, Basler CF. Propagation, Inactivation, and Safety Testing of SARS-CoV-2. *Viruses.* 2020;12(6):622. doi:10.3390/v12060622
  27. INS. Manual de procedimientos para diagnóstico del virus de la inmunodeficiencia humana tipo 1 (VIH-1) por inmunofluorescencia indirecta - Informes y publicaciones - Ministerio de Salud - Gobierno del Perú [Internet]. 2001 [cited 2023 Feb 2]. Available from: <https://www.gob.pe/institucion/minsa/informes-publicaciones/353005-manual-de-procedimientos-para-diagnostico-del-virus-de-la-inmunodeficiencia-humana-tipo-1-vih-1-por-inmunofluorescencia-indirecta>
  28. Thermo Fisher Scientific. SuperScript™ IV One-Step RT-PCR System [Internet]. 2022 [cited 2023 Feb 2]. Available from: <https://www.thermofisher.com/order/catalog/product/12594025>
  29. Wood DE, Lu J, Langmead B. Improved metagenomic analysis with Kraken 2. *Genome Biol.* 2019; 20(1):1-13. doi:10.1186/S13059-019-1891-0/FIGURES/2
  30. Goswami C, Sheldon M, Bixby C, Keddache M, Bogdanowicz A, Wang Y, *et al.* Identification of SARS-CoV-2 variants using viral sequencing for the Centers for Disease Control and Prevention genomic surveillance program. *BMC Infect Dis.* 2022; 22(1):404. doi:10.1186/S12879-022-07374-7
  31. Li H, Durbin R. Fast and accurate short read alignment with Burrows-Wheeler transform. *Bioinformatics.* 2009; 25(14):1754-60. doi:10.1093/BIOINFORMATICS/BTP324
  32. Danecek P, Bonfield JK, Liddle J, Marshall J, Ohan V, Pollard MO, *et al.* Twelve years of SAMtools and BCFtools. *Gigascience.* 2021;10(2):giab008. doi:10.1093/gigascience/giab008
  33. Grubaugh ND, Gangavarapu K, Quick J, Matteson NL, De Jesus JG, Main BJ, *et al.* An amplicon-based sequencing framework for accurately measuring intrahost virus diversity using PrimalSeq and iVar. *Genome Biol.* 2019; 20(1):1-19. doi: 10.1186/S13059-018-1618-7/FIGURES/9
  34. Stamatakis A. RAxML version 8: a tool for phylogenetic analysis and post-analysis of large phylogenies. *Bioinformatics.* 2014; 30(9):1312-3. doi: 10.1093/BIOINFORMATICS/BTU033
  35. Singanayagam A, Patel M, Charlett A, Bernal JL, Saliba V, Ellis J, *et al.* Duration of infectiousness and correlation with RT-PCR cycle threshold values in cases of COVID-19, England, January to May 2020. *Euro Surveill.* 2020;25(32):2001483. doi:10.2807/1560-7917.ES.2020.25.32.2001483
  36. Araujo DB, Machado RRG, Amgarten DE, Malta F de M, de Araujo GG, Monteiro CO, *et al.* SARS-CoV-2 isolation from the first reported patients in Brazil and establishment of a coordinated task network. *Mem Inst Oswaldo Cruz.* 2020;115:1-8. doi: 10.1590/0074-027620200342
  37. Francis R, Le Bideau M, Jardot P, Grimaldier C, Raoult D, Bou Khalil JY, *et al.* High-speed large-scale automated isolation of SARS-CoV-2 from clinical samples using miniaturized co-culture coupled to high-content screening. *Clin Microbiol Infect.* 2021; 27(1):128.e1-128.e7. doi:10.1016/J.CMI.2020.09.018
  38. Chung H, Noh JY, Koo BS, Hong JJ, Kim HK. SARS-CoV-2 mutations acquired during serial passage in human cell lines are consistent with several of those found in recent natural SARS-CoV-2 variants. *Comput Struct Biotechnol J.* 2022; 20:1925-34. doi: 10.1016/J.CSBJ.2022.04.022
  39. Ogando NS, Dalebout TJ, Zevenhoven-Dobbe JC, Limpens RWAL, van der Meer Y, Caly L, *et al.* SARS-coronavirus-2 replication in Vero E6 cells: Replication kinetics, rapid adaptation and cytopathology. *J Gen Virol.* 2020; 101(9):925-40. doi: 10.1099/JGV.0.001453/CITE/REFWORKS
  40. Sonnleitner ST, Sonnleitner S, Hinterbichler E, Halbfurter H, Kopecky DBC, Koblmüller S, *et al.* The mutational dynamics of the SARS-CoV-2 virus in serial passages *in vitro*. *Virology.* 2022; 37(2):198-207. doi: 10.1016/J.VIRS.2022.01.029
  41. Sasaki M, Uemura K, Sato A, Toba S, Sanaki T, Maenaka K, *et al.* SARS-CoV-2 variants with mutations at the S1/S2 cleavage site are generated *in vitro* during propagation in TMPRSS2-deficient cells. *PLOS Pathog.* 2021; 17(1):e1009233. doi:10.1371/JOURNAL.PPAT.1009233